Turkish Journal of Electrical Engineering and Computer Sciences

Volume 24 | Number 4 Article 15

1-1-2016

Modeling and control of a 6-control-area interconnected power system to protect the network frequency applying different controllers

NGOCKHOAT NGUYEN

QI HUANG

THI-MAI-PHUONG DAO

Turkish Journal of Electrical Engineering & Computer Sciences

http://journals.tubitak.gov.tr/elektrik/

Research Article

Turk J Elec Eng & Comp Sci
(2016) 24: 2205 – 2219

doi:10.3906/elk-1403-78

Modeling and control of a 6-control-area interconnected power system to protect the network frequency applying different controllers

NgocKhoat NGUYEN[1,*], Qi HUANG[1], Thi-Mai-Phuong DAO[2]

[1]School of Energy Science and Engineering, University of Electronic Science and Technology of China, Chengdu, Sichuan, P.R. China

[2]College of Electrical and Information Engineering, Hunan University, Changsha, Hunan, P.R. China

Received: 10.03.2014 • **Accepted/Published Online:** 05.07.2014 • **Final Version:** 15.04.2016

Abstract: Modern and large power systems, which are normally composed of several interconnected generating stations (multiarea), have complex and diverse structures in practice. It is necessary to deal with the automatic generation control to ensure the stability, continuity, and economy of the generation schedule in a power grid. For the automatic generation control strategy, the most important goal is to protect the network frequency from load variations, which can appear randomly in any area. As a result, it is essential to design efficient controllers applied to multiarea interconnected power systems in order to maintain the network frequency at the nominal values (50 Hz or 60 Hz), and keep the tie-line power flow at the scheduled MW.

In this paper, we first analyze and build a model of the 6-control-area interconnected power system as the typical case study. Subsequently, different frequency controllers based on tie-line bias control strategy, namely integral, proportional–integral, proportional–integral–derivative, and PI-based fuzzy logic, will be investigated and applied to the power system model. The most important control performances, such as overshoots and settling times, are considered in this study to evaluate the stability of the power system and choose the most suitable controller for maintaining the network frequency.

The simulation results have been achieved by using MATLAB/Simulink package version 2013 in this work. According to these results, the maximum overshoots of the PI-based fuzzy logic controller are from 36.56% to 90.13%, and its settling times are from 19.00% to 98.26% in comparison with the other regulators in the given control power system. Therefore, the PI-based fuzzy logic controller has been chosen as the best control solution to bring the grid frequency back to its nominal value as quickly as possible after occurrence of load variations.

Key words: Interconnected power system, deviation, frequency, tie-line power, I, PI, PID, fuzzy logic

1. Introduction

In a modern and large power system, a lot of generating stations are interconnected by tie-lines to exchange MW among them. These stations are also defined as generating areas (or control areas). During the operation of the above multiarea interconnected power system, loads at any station can appear randomly and changeably based on the behavior of users; thus the frequency in the network will deviate from the nominal values (50 Hz or 60 Hz). Because of the close relationship between the frequency and the active power in a network, this deviation causes a change in the generation demand [1,2]. Therefore, it is necessary to establish robust load

*Correspondence: khoatnn@epu.edu.vn

frequency control strategies to regulate the automatic generation in an interconnected power system [3–5]. In general, the main roles of these control strategies are to maintain the stability of the system frequency and tie-line power to ensure the optimal and economical generation of a power network in reality.

In order to achieve the above control objectives, three control strategies, namely flat frequency, flat tie-line power, and tie-line bias control schemes, can be applied. According to [2], flat frequency controllers are only applied effectively for a case of a power system composed of a very small generating area and a very large network. It is a fact that load changes in the much smaller area may not significantly impact on the whole system frequency. This leads to limited applications of this control technique due to the complexity and diversity of the modern and large power systems nowadays. On the other hand, flat tie-line power controllers can only be used in combination with flat frequency controllers. However, the obtained control results still do not reach the desired performances. For the best choice, the tie-line bias control strategy has been used widely, practically, and efficiently to achieve the required control objectives. In principle, this control strategy uses the combination of both the frequency and tie-line power deviations, namely, area control errors (ACEs), as input signals [6,7]. As a result, these deviations can be reduced under permissible tolerances. Moreover, the first two control strategies as mentioned above are only the particular and limited cases of the tie-line bias control scheme when the bias reaches zero and infinite values, respectively. Hence, the third control strategy covers all of the dominant characteristics of the previous methods.

In fact, 2 types of controllers based on the tie-line bias control strategy have been applied, namely conventional and intelligent controllers. Traditionally, conventional controllers using the integral (I), proportional–integral (PI), or proportional–integral–derivative (PID) regulators are initially used to damp the transients of both the network frequency and tie-line power deviations. However, when applying these controllers, control systems have only obtained very poor performances, such as high overshoots and long settling times, which have strongly affected the operation and stability of the system [8–10]. To overcome these drawbacks, intelligent controllers using modern control techniques [11–14], e.g., fuzzy logic (FL), have been investigated widely in recent years. By using the FL controllers, the above control performances can be significantly improved in order to achieve the desired characteristics.

In this paper, different controllers, namely, I, PI, PID, and PI-based FL, are successfully investigated and compared to demonstrate the effectiveness of the tie-line bias control strategy used in the working frequency maintenance of a power system. A 6-control-area nonreheat interconnected power system is built as a typical case study to apply the above controllers. The definition of a control area has been used to imply that each generating area includes not only a generator but also several generators connected in parallel to supply the power demand. These generators can be treated as a coherent group or an equivalent generator to establish the frequency control strategies. From the evaluation of simulation results obtained by using the MATLAB/Simulink package, PI-based FL controllers are selected as an efficient solution to the given control issue.

In the next section of this paper, the model of a 6-control-area interconnected power system will be built corresponding to the tie-line bias control strategy. Section 3 then presents the application of different controllers, namely conventional and intelligent controllers, based on the proposed control scheme. Finally, simulation results and discussions will be given in the following 2 sections to evaluate and choose the most efficient controller to stabilize the network frequency.

2. Modeling of a 6-control-area interconnected power system

In the context of this work, a typical case study of a multiarea interconnected power system consisting of 6 generating areas will be designed. Figure 1 shows simple architectures of a 6-control-area interconnected power system. As shown in Figures 1a and 1b, each control area is interconnected with 2, 3, or 4 other areas to exchange the power demand. Figure 1c describes the other case where only the 6th control area is interconnected with each other area to exchange the scheduled MW. In Figure 1d, each generating area is interconnected with 5 other areas; hence load changes can appear randomly at any area, and affect the local frequencies as well as the tie-line power flows. As a result, the frequency and tie-line power deviations generated need to be damped by applying effective controllers in each area.

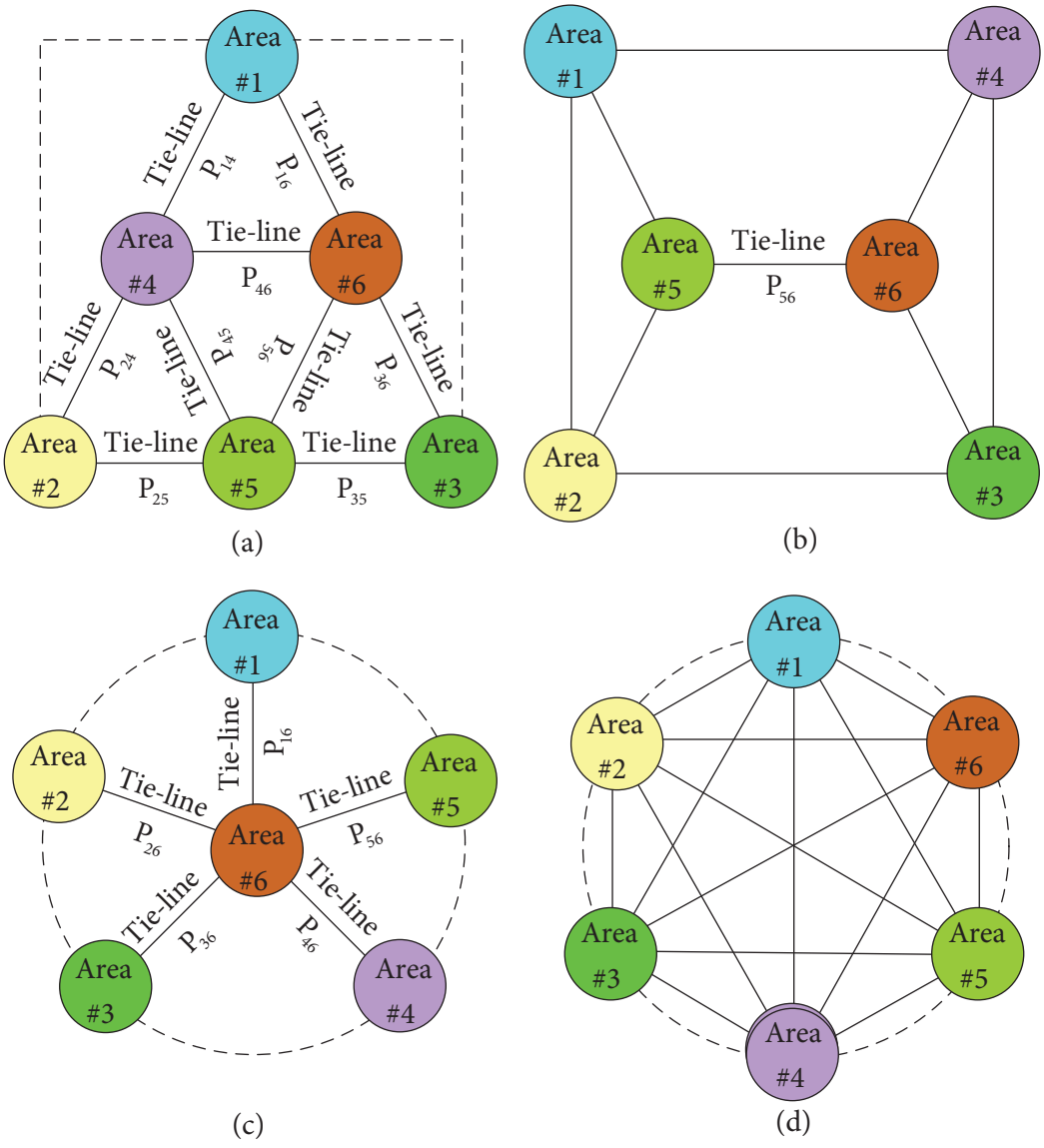

Figure 1. 6-control-area interconnected power system models: (a) Control areas #1, #2, and #3 are interconnected with 2 other areas; (b) Each control area is interconnected with 3 other control areas; (c) Control area #6 is interconnected with each other control area; (d) Each control area is interconnected with each other control area.

In this work, tie-line bias control based controllers are used for each area to solve this problem [1–5]. For the typical case study, the fourth architecture of the power grid as indicated in Figure 1d is used in this work. The other cases can also be implemented in a similar manner. The corresponding structure of the control area $\#i$ is presented in Figure 2.

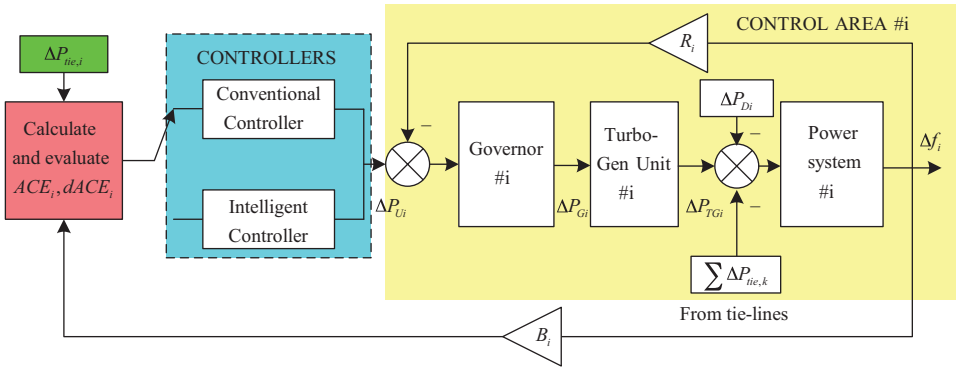

Figure 2. The structure of the control area $\#i$ using different controllers.

As mentioned earlier, each control area is simply composed by a group of governors, equivalent turbine-generator units, and demand loads. The corresponding transfer functions of an equivalent governor and nonreheat turbine-generator unit in each control area as shown in Figure 2 are expressed below [2]

$$G_{Gi}(s) = \frac{1}{s.T_{Gi} + 1} \tag{1}$$

$$G_{TGi}(s) = \frac{1}{s.T_{TGi} + 1}, \tag{2}$$

where T_{Gi} and T_{TGi}, in s, are governor and nonreheat turbine time constants, respectively. To convert the power deviation of the generator and load into the frequency change [1,2,15], a transfer function corresponding to the *Power System* $\#i$ block in Figure 2 can be given as follows:

$$G_{Pi}(s) = \frac{K_{pi}}{s.T_{Pi} + 1}, \tag{3}$$

where K_{pi}, in *Hz/pu.MW*, and T_{Pi}, in s, are the characteristic constants for the ith control area.

In order to use this model in future control strategies, a state space model will be built in this work. By extending the idea in [2], we can design the corresponding state space model of the given 6-control-area interconnected power system as expressed in the following equations (in both Laplace and time domains)

$$\Delta F_i(s) = \frac{K_{Pi}}{sT_{Pi} + 1} \left[\Delta P_{TGi}(s) - \Delta P_{Di}(s) - \Delta P_{Tie,i}(s)\right] \tag{4}$$

$$\Delta P_{TGi}(s) = \frac{1}{sT_{TGi} + 1} \Delta P_{Gi}(s) \tag{5}$$

$$\Delta P_{Gi}(s) = \frac{1}{sT_{Gi}+1}\left[\Delta P_{Ui}(s) - \frac{1}{R_i}\Delta F_i(s)\right] \tag{6}$$

$$\Delta P_{tie,i}(s) = \frac{2\pi}{s}\sum_{j=1,j\neq i}^{6} T_{ij}\left[\Delta F_i(s) - \Delta F_j(s)\right] \tag{7}$$

$$\Delta \dot{f}_i(t) = \frac{K_{Pi}}{T_{Pi}}\left[-\frac{1}{K_{Pi}}\Delta f_i(t) + \Delta P_{TGi}(t) - \Delta P_{Di}(t) - \Delta P_{Tie,i}(t)\right] \tag{8}$$

$$\Delta \dot{P}_{TGi}(t) = \frac{1}{T_{TGi}}\left[-\Delta P_{TGi}(t) + \Delta P_{Gi}(t)\right] \tag{9}$$

$$\Delta \dot{P}_{Gi}(t) = \frac{1}{T_{Gi}}\left[-\Delta P_{Gi}(t) + \Delta P_{Ui}(t) - \frac{1}{R_i}\Delta f_i(t)\right] \tag{10}$$

$$\Delta \dot{P}_{tie,i}(t) = 2\pi\sum_{j=1,j\neq i}^{6} T_{ij}\left[\Delta f_i(t) - \Delta f_j(t)\right]. \tag{11}$$

From (8), (9), (10), and (11), a state space model in a corresponding matrix form can be established as follows:

$$\dot{X} = AX + BU + FD, \tag{12}$$

where X is a state variable vector,

$$X = \begin{bmatrix} X_1 \\ X_2 \\ X_3 \\ X_4 \end{bmatrix} \text{ with } \begin{cases} X_1 = [\Delta f_1(t),\ \Delta f_2(t),\ \Delta f_3(t),\ \Delta f_4(t),\ \Delta f_5(t),\ \Delta f_6(t)]^T \\ X_2 = [\Delta P_{TG1}(t),\ \Delta P_{TG2}(t),\ \Delta P_{TG3}(t),\ \Delta P_{TG4}(t),\ \Delta P_{TG5}(t),\ \Delta P_{TG6}(t)]^T \\ X_3 = [\Delta P_{G1}(t),\ \Delta P_{G2}(t),\ \Delta P_{G3}(t),\ \Delta P_{G4}(t),\ \Delta P_{G5}(t),\ \Delta P_{G6}(t)]^T \\ X_2 = [\Delta P_{Tie1}(t),\ \Delta P_{Tie2}(t),\ \Delta P_{Tie3}(t),\ \Delta P_{Tie4}(t),\ \Delta P_{Tie5}(t),\ \Delta P_{Tie6}(t)]^T \end{cases};$$

U is an input signal vector,

$$U = [P_{U1}(t), P_{U2}(t), P_{U3}(t), P_{U4}(t), P_{U5}(t), P_{U6}(t)]^T;$$

D is a vector of load variations,

$$D = [\Delta P_{D1}(t), \Delta P_{D2}(t), \Delta P_{D3}(t), \Delta P_{D4}(t), \Delta P_{D5}(t), \Delta P_{D6}(t)]^T;$$

A, B, F are the state matrices,

$$A = \begin{bmatrix} A1 \\ A2 \\ A3 \\ A4 \end{bmatrix},$$

$$A_1 = \begin{bmatrix} \frac{-1}{T_{P1}} & & \underline{O}(1,5) & \frac{K_{P1}}{T_{P1}} & \underline{O}(1,11) & \frac{-K_{P1}}{T_{P1}} & \underline{O}(1,5) \\ \underline{O}(1,1) & \frac{-1}{T_{P2}} & \underline{O}(1,5) & \frac{K_{P2}}{T_{P2}} & \underline{O}(1,11) & \frac{-K_{P2}}{T_{P2}} & \underline{O}(1,4) \\ \underline{O}(1,2) & \frac{-1}{T_{P3}} & \underline{O}(1,5) & \frac{K_{P3}}{T_{P3}} & \underline{O}(1,11) & \frac{-K_{P3}}{T_{P3}} & \underline{O}(1,3) \\ \underline{O}(1,3) & \frac{-1}{T_{P4}} & \underline{O}(1,5) & \frac{K_{P4}}{T_{P4}} & \underline{O}(1,11) & \frac{-K_{P4}}{T_{P4}} & \underline{O}(1,2) \\ \underline{O}(1,4) & \frac{-1}{T_{P5}} & \underline{O}(1,5) & \frac{K_{P5}}{T_{P5}} & \underline{O}(1,11) & \frac{-K_{P5}}{T_{P5}} & \underline{O}(1,1) \\ \underline{O}(1,5) & \frac{-1}{T_{P6}} & \underline{O}(1,5) & \frac{K_{P6}}{T_{P6}} & \underline{O}(1,11) & \frac{-K_{P6}}{T_{P6}} & \end{bmatrix};$$

$\underline{O}(m,n)$ is a $m \times n$ zero matrix;

$$A_2 = \begin{bmatrix} \underline{O}(1,6) & \frac{-1}{T_{TG1}} & \underline{O}(1,5) & \frac{1}{T_{TG1}} & \underline{O}(1,11) \\ \underline{O}(1,7) & \frac{-1}{T_{TG2}} & \underline{O}(1,5) & \frac{1}{T_{TG2}} & \underline{O}(1,10) \\ \underline{O}(1,8) & \frac{-1}{T_{TG3}} & \underline{O}(1,5) & \frac{1}{T_{TG3}} & \underline{O}(1,9) \\ \underline{O}(1,9) & \frac{-1}{T_{TG4}} & \underline{O}(1,5) & \frac{1}{T_{TG4}} & \underline{O}(1,8) \\ \underline{O}(1,10) & \frac{-1}{T_{TG5}} & \underline{O}(1,5) & \frac{1}{T_{TG5}} & \underline{O}(1,7) \\ \underline{O}(1,11) & \frac{-1}{T_{TG6}} & \underline{O}(1,5) & \frac{1}{T_{TG6}} & \underline{O}(1,6) \end{bmatrix};$$

$$A_3 = \begin{bmatrix} \frac{-1}{R_1 T_{G1}} & \underline{O}(1,11) & \frac{-1}{T_{G1}} & \underline{O}(1,11) & \\ \underline{O}(1,1) & \frac{-1}{R_2 T_{G2}} & \underline{O}(1,11) & \frac{-1}{T_{G2}} & \underline{O}(1,10) \\ \underline{O}(1,2) & \frac{-1}{R_3 T_{G3}} & \underline{O}(1,11) & \frac{-1}{T_{G3}} & \underline{O}(1,9) \\ \underline{O}(1,3) & \frac{-1}{R_4 T_{G4}} & \underline{O}(1,11) & \frac{-1}{T_{G4}} & \underline{O}(1,8) \\ \underline{O}(1,4) & \frac{-1}{R_5 T_{G5}} & \underline{O}(1,11) & \frac{-1}{T_{G5}} & \underline{O}(1,7) \\ \underline{O}(1,5) & \frac{-1}{R_6 T_{G6}} & \underline{O}(1,11) & \frac{-1}{T_{G6}} & \underline{O}(1,6) \end{bmatrix};$$

$$A_4 = \begin{bmatrix} \sum_{k=2}^{6} T_{1k} & -T_{12} & -T_{13} & -T_{14} & -T_{15} & -T_{16} & \underline{O}(1,18) \\ -T_{21} & \sum_{k=1,k\neq 2}^{6} T_{2k} & -T_{23} & -T_{24} & -T_{25} & -T_{26} & \underline{O}(1,18) \\ -T_{31} & -T_{32} & \sum_{k=1,k\neq 3}^{6} T_{3k} & -T_{34} & -T_{35} & -T_{36} & \underline{O}(1,18) \\ -T_{41} & -T_{42} & -T_{43} & \sum_{k=1,k\neq 4}^{6} T_{4k} & -T_{45} & -T_{46} & \underline{O}(1,18) \\ -T_{51} & -T_{52} & -T_{53} & -T_{54} & \sum_{k=1,k\neq 5}^{6} T_{5k} & -T_{56} & \underline{O}(1,18) \\ -T_{61} & -T_{62} & -T_{63} & -T_{64} & -T_{65} & \sum_{k=1}^{5} T_{6k} & \underline{O}(1,18) \end{bmatrix};$$

$$B = \begin{bmatrix} \underline{O}(1,12) & \frac{1}{T_{G1}} & \underline{O}(1,11) \\ \underline{O}(1,13) & \frac{1}{T_{G2}} & \underline{O}(1,10) \\ \underline{O}(1,14) & \frac{1}{T_{G3}} & \underline{O}(1,9) \\ \underline{O}(1,15) & \frac{1}{T_{G4}} & \underline{O}(1,8) \\ \underline{O}(1,16) & \frac{1}{T_{G5}} & \underline{O}(1,7) \\ \underline{O}(1,17) & \frac{1}{T_{G6}} & \underline{O}(1,6) \end{bmatrix}^T \text{ and } F = \begin{bmatrix} \frac{-K_{P1}}{T_{P1}} & & \underline{O}(1,23) \\ \underline{O}(1,1) & \frac{-K_{P2}}{T_{P2}} & \underline{O}(1,22) \\ \underline{O}(1,2) & \frac{-K_{P3}}{T_{P3}} & \underline{O}(1,21) \\ \underline{O}(1,3) & \frac{-K_{P4}}{T_{P4}} & \underline{O}(1,20) \\ \underline{O}(1,4) & \frac{-K_{P5}}{T_{P5}} & \underline{O}(1,19) \\ \underline{O}(1,5) & \frac{-K_{P6}}{T_{P6}} & \underline{O}(1,18) \end{bmatrix}^T.$$

When applying the tie-line bias control technique, the input of the corresponding controller used for the ith control area is defined as

$$ACE_i(s) = \Delta P_{tie,i}(s) + B_i.\Delta F_i(s). \tag{13}$$

In (13), $B_i = D_i + \frac{1}{R_i}$ is the frequency bias factor [1–6]; D_i, R_i, and $ACE_i(s)$ are the load damping factor, the generator speed regulation, and the area control error of the ith control area, respectively. By using this definition, only 1 controller is necessary for an area to extinguish the deviations of both the frequency and tie-line power flow in accordance with the principle of the tie-line bias control. Therefore, this control method is applied in this work in order to stabilize the network frequency. Figure 3 describes a full model of a 6-control-area power system built in the MATLAB/Simulink environment. This model will be used for simulation process as discussed in Section 4 of this paper.

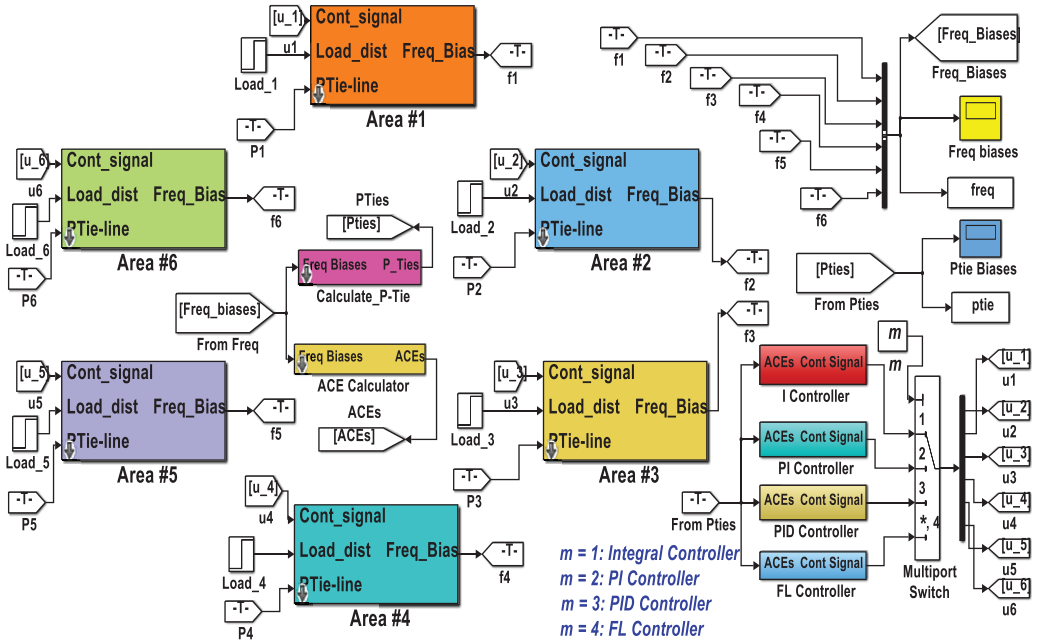

Figure 3. A 6-control-area interconnected power system model built in MATLAB/simulink environment.

3. Tie-line bias control strategy-based controllers

3.1. Conventional controllers

Basically, an integral controller with the gain K_{Ii} can be applied to the ith area as 1 conventional regulator. Based on the tie-line bias control strategy, the principle of this controller can be given as follows:

$$u_i(t) = K_{Ii} \int ACE_i(t)dt = K_{Ii} \int (\Delta P_{tie,i}(t) + B_i.\Delta f_i(t))dt, \tag{14}$$

$$U_i(s) = \frac{K_{Ii}}{s} ACE_i(s) = \frac{K_{Ii}}{s} \left(\Delta P_{tie,i}(s) + B_i.\Delta F_i(s)\right). \tag{15}$$

In (14) and (15), U_i is the control signal that will be fed to the control area $\#i$. The gain constant of the above controller, K_{Ii}, must be defined to satisfy both conditions of the systematically dynamic response, namely the fast transient restoration and the low overshoot. According to some studies [3,5,10], the dynamic response of

this controller is too slow to stabilize multi-interconnected power networks that comprise nonlinear elements. Consequently, it is essential to improve this controller in order to achieve better control performances.

The second category of conventional controller that can be considered to solve the problem of frequency maintenance is PID regulator. It is well known that PID controllers have been widely and effectively used in control systems [16–18]. In addition, they are more useful to be applied in the tie-line bias control strategy for the frequency stability against the load variations in a power network. Basically, the principle of this controller is similar to that of the integral regulator as presented below

$$\begin{aligned} u_i(t) &= K_{pi}.ACE_i(t) + K_{Ii}\int_0^t ACE_i(\tau)d\tau + K_{Di}\frac{d}{dt}ACE_i(t) \\ &= K_{pi}\left(ACE_i(t) + \frac{1}{T_{Ii}}\int_0^t ACE_i(\tau)d\tau + T_{Di}\frac{d}{dt}ACE_i(t)\right), \end{aligned} \tag{16}$$

$$U_i(s) = K_{Pi}\left(1 + \frac{1}{sT_{Ii}} + sT_{Di}\right)ACE_i(s) \tag{17}$$

where $K_{pi}, K_{Ii}, K_{di}, T_{Ii}$, and T_{Di} are proportional, integral, derivative gain factors, integral time, and derivative time constants, respectively.

According to [18–20], the performance characteristics of a control system are strongly affected by the above gain coefficients as mentioned below

1. the larger the proportional gain, the smaller the steady state error; however, the control loop also becomes unstable,
2. the shorter the integral time, the more impetuous the implementation of an integral is, and
3. the larger the derivative coefficient, the more changeable the error becomes.

With these effects, it is essential to consider tuning methods of K_P, K_D, and K_I in control systems applying PID controllers [18–22]. In this work, we have used the Ziegler–Nichols method [15,20–23] to tune these coefficients. By applying this method, the integral and derivative gains are first set to zero values; then the proportional gain is tuned to reach the value at which the output of the system begins to fluctuate. In the second step, the derivative gain will be defined with the proportional gain tuned above to make sure that the transient performances are obtained. In the last step, the integral gain will be fixed with the other factors chosen above to ensure the steady state characteristic of the control system. Because the derivative action is too sensitive to reach the steady state, a PI (proportional–integral) controller can be used to replace a PID regulator in a control system. It is very easy to design a PI controller from a PID regulator by setting a zero derivative coefficient ($K_{Di} = 0$). In this study, the performances of such PI controllers applied to the frequency maintenance will also be presented in comparison with those of the other regulators.

3.2. Intelligent controller

In practice, a large-scale multiarea interconnected power system has nonlinear characteristics; thus a conventional controller should be replaced effectively by an intelligent controller using the FL technique. According to [3,10,24–26], a FL controller cannot be affected by the parameters of a control system, particularly in a power network. Moreover, it has the following dominant advantages:

1. it is very efficient to use the incomplete information to make a control decision for the control system,

2. it is very flexible to make any control decision by applying the FL controller, and
3. FL controllers applied in a control system can provide an effective human machine interface (HMI) for users.

Since FL controllers may not require the estimation of parameters, these parameters can vary very fast in a control system. Meanwhile, FL controllers still act effectively to obtain the desired control performances [10,24,25]. Thus, such FL controllers have been applied more usefully in industrial control systems as well as in multiarea power networks to carry out frequency stability.

Figure 4 describes the principle of a FL controller used for the ith control area. Based on the tie-line bias control scheme, there are a total of 6 FL controllers used in the control system. Each FL controller, as depicted in Figure 4, has been fed by 2 input signals, ace_i and the derivative of ace_i, $\mathrm{d}ace_i$, relating to ACE_i and its derivative, $\mathrm{d}ACE_i$, as described below

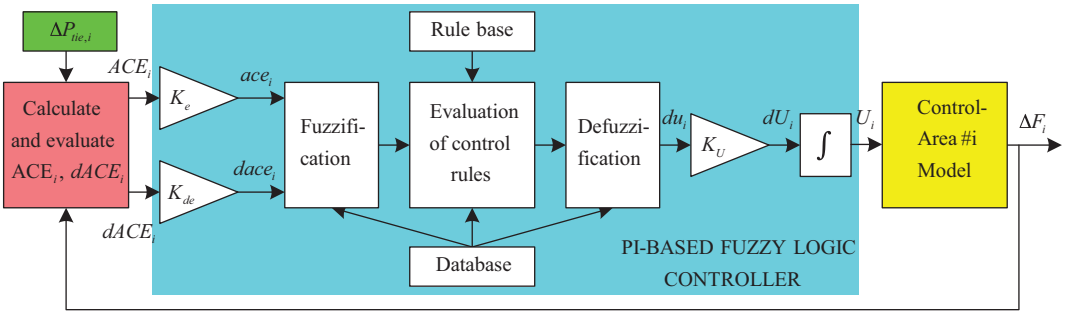

Figure 4. The structure of the PI-based FL controller for the control area # i.

$$ace_i(t) = \frac{1}{Ke_i} ACE_i(t) = \frac{1}{Ke_i} \left(\Delta P_{tie,i}(t) + B_i \Delta f_i(t)\right) \tag{18}$$

$$dace_i(t) = \frac{1}{Kde_i} \frac{d}{dt} ACE_i(t) = \frac{1}{Kde_i} \frac{d}{dt} \left(\Delta P_{tie,i}(t) + B_i \Delta f_i(t)\right), \tag{19}$$

where Ke_i and Kde_i are the correct coefficients corresponding to ACE_i and the derivative of ACE_i. The output of the given controller is du_i relating to the control signal or the power change reference of the ith control area, $\Delta P_{ref,\,i}$, by the proportional factor Ku_i and the summation (or integral) of dU_i (see Figure 4). In general, each FL controller is an input/output static nonlinear mapping and thus the principle of the proposed FL controller can be written as follows:

$$du_i(t) = K_1.ace_i(t) + K_2.dace_i(t); \tag{20}$$

hence,

$$u_i(t) = \int du_i(t)dt = K_1 \int ace_i(t)dt + K_2.ace_i(t), \tag{21}$$

where K_1 and K_2 are gain coefficients. From (18), (19), and (21), we can infer the following formulas:

$$U_i(t) = Ku_i.u(t) = Ku_i \left[\frac{K_1}{Ke_i} \int ACE_i(t)dt + \frac{K_2}{Kde_i}.ACE_i(t)\right] \tag{22}$$

and

$$U_i(t) = K_P.ACE_i(t) + K_I. \int ACE_i(t)dt. \tag{23}$$

From (23), it can be clearly seen that the principle of the proposed FL controller is similar to that of the PI regulator as mentioned earlier. As a result, the FL controller used can be defined as a PI-based FL controller [11,13,27].

Basically, there are three processes of a PI-based FL controller [10–14]: fuzzification, evaluation of control rule base, and defuzzification, as illustrated in Figure 4. For the control rule base of the above FL controller, a 49-rule base is used in our work. This rule base designed is based on the understanding of the control system in order to minimize the frequency and tie-line power flow changes. This leads to a simple control rule in the proposed controller as follows:

IF *the first input, $ace_i(t)$, is near zero* AND *the second input, $dace_i(t)$, is positive small,* THEN *the corresponding output, du_i, is negative small.*

A full rule base is illustrated in Table 1 with 7 MFs for $ace_i(t)$ and $dace_i(t)$ and 9 MFs for $du_i(t)$ as indicated in Figure 5.

Table 1. Rule matrix for the proposed FL controller.

$dace_i(t)$	$ace_i(t)$						
	NB	NM	NS	ZE	PS	PM	PB
NB	NB	NB	NB	NM	NS	NVS	ZE
NM	NB	NB	NM	NS	NVS	ZE	PVS
NS	NB	NM	NS	NVS	ZE	PVS	PS
ZE	NM	NS	NVS	ZE	PVS	PS	PM
PS	NS	NVS	ZE	PVS	PS	PM	PB
PM	NVS	ZE	PVS	PS	PM	PB	PB
PB	ZE	PVS	PS	PM	PB	PB	PB

NB – Negative Big, NVS – Negative Very Small, NM – Negative, NS – Negative Small, ZE – Zero, PVS – Positive Very Small, PS – Positive Small, PM – Positive Medium, PB – Positive Big

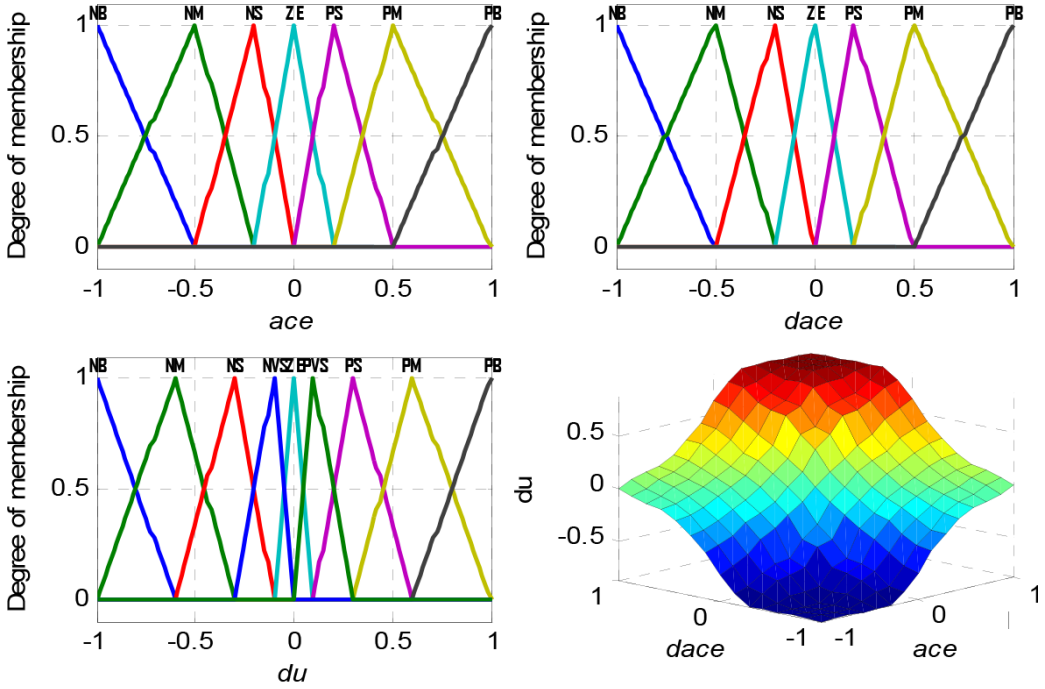

Figure 5. Degree of membership functions and the 3D surface of the given FL controller.

In this design, the MAX–MIN composition is used in which each output, MF, is obtained by a MIN operator. Meanwhile, a MAX operator has been used for the corresponding fuzzy logic output [27]. Furthermore, this operation is illustrated in Figure 5 as the 3D membership surface. To verify the effectiveness of this control strategy, the next section will carry out the simulation processes using the MATLAB/Simulink package.

4. Simulation results

In this study, 4 simulated cases of regulators are considered, namely I, PI, PID, and PI-based FL controller. In order to evaluate the effectiveness of different controllers based on the tie-line bias control strategy mentioned earlier, a condition of step-load changes is fed to all simulation cases at the starting time of zero as given below

$$\begin{aligned} D &= [\Delta P_{D1},\ \Delta P_{D2},\ \Delta P_{D3},\ \Delta P_{D4},\ \Delta P_{D5},\ \Delta P_{D6}]^T \\ &= [2(\%),\ 1(\%),\ 1.2(\%),\ 1.5(\%),\ 0(\%),\ 1(\%)]^T \end{aligned}, \tag{24}$$

where ΔP_{Di} is the load change in the corresponding control area $\#i$. Our control objective is to adjust the state vector $X_{FP} = [\Delta f_i,\ \ \Delta P_{tie,i}]^T$, which has to converge towards the zero-steady state $X^0_{FP} = [\underline{O}(1,6),\ \underline{O}(1,6)]^T$ with the best control characteristics, such as the smallest overshoots and the shortest settling times. By using the MATLAB/Simulink package, simulation results have been obtained. Figure 6 illustrates the frequency deviations of the 1st and 6th control areas, corresponding to the application of I and PID controllers in the given control system. Figure 7 shows the frequency deviations of the above areas using PI and FL controllers. Figure 8 plots the tie-line power deviations of the 2nd and 3rd areas for three cases: I, PI, and PID controller.

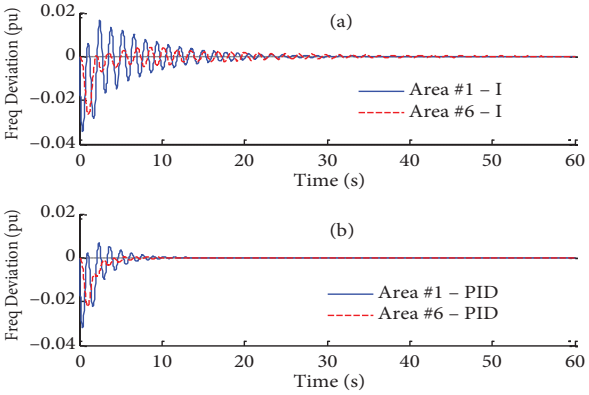

Figure 6. Frequency deviations of the 1st and 6th control areas using I and PID controllers.

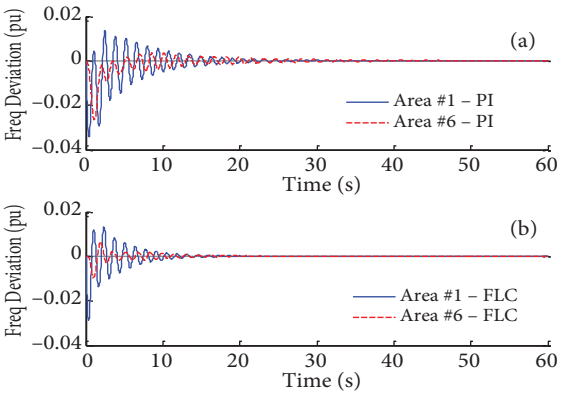

Figure 7. Frequency deviations of the 1st and 6th control areas using PI and PI-FL controllers.

The following figures present a comparison of the different controllers used above. Figure 9a indicates the response of frequency deviation using different controllers only for the first area. By calculating the frequency deviation errors of the above controllers, Figure 9b plots the corresponding error curves. As shown in this figure, the frequency change error between I-PID controllers is the smallest, whereas the bias of I-FL controllers is the largest. Figures 10 and 11 indicate the absolute values of the first overshoots and the settling times of all control areas using different types of controllers. In Figure 11, a permissible frequency tolerance of 0.1% for the comparison aim of the proposed controllers is given.

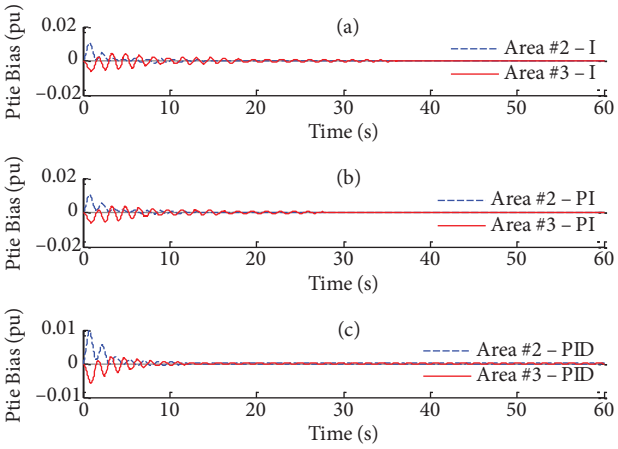

Figure 8. Tie line power deviations of the 2nd and 3rd control areas.

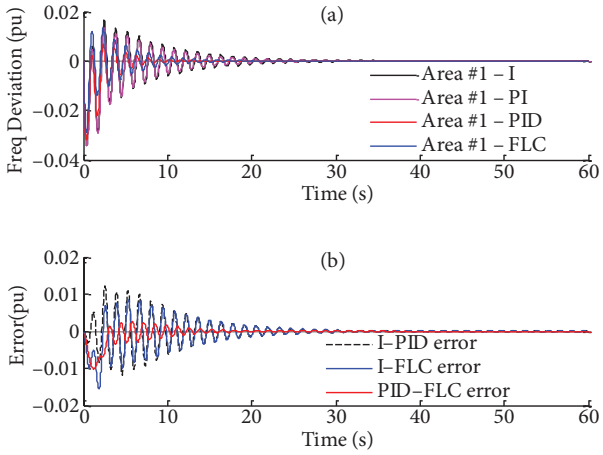

Figure 9. Comparison of the given controllers for the control area #1: (a) Different controllers used in the control area #1; (b) Frequency deviation errors.

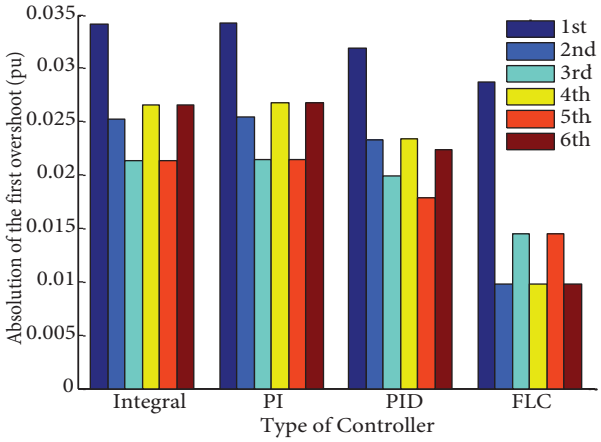

Figure 10. The absolution of the first overshoots of all control areas.

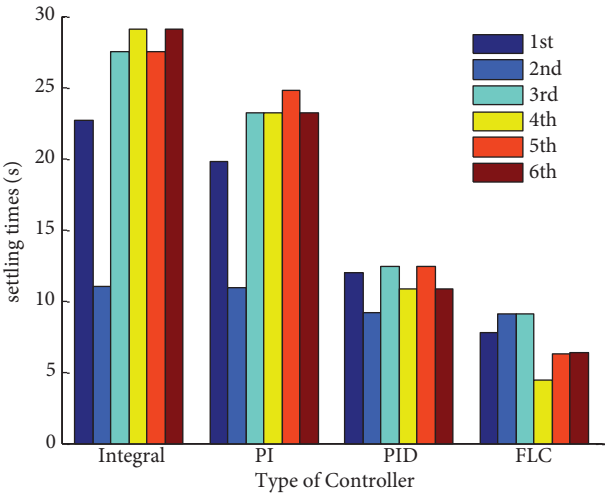

Figure 11. The settling times of all control areas corresponding to the acceptable frequency tolerance of 0.1%.

Furthermore, to demonstrate numerically the obtained results, Tables 2 and 3 represent comparisons of the PI-based FL controller with the other controllers for all control areas. According to Table 2, the first overshoots of the FL controller dynamic response are approximate from 36.56% to 90.13% in comparison with those of the other controllers. In addition, the corresponding settling times are approximated from 19% to 98.26% compared with the conventional controllers. These results verify that both the first overshoot (the maximum overshoot) and the settling time of the PI-based FL controller are much smaller than those of the other controllers. Consequently, PI-based FL controllers have achieved the better control performances compared with the conventional controller. This leads to the best choice of the FL frequency controller based on PI principle for the most efficient solution of the frequency maintenance problem.

Table 2. The comparison of the first overshoot, in percent. The results of the PI-based FL controller are much smaller than those of the other regulators (from 36.5578% to 90.1321%) to demonstrate the efficient control performance of the proposed FL controller.

Controller	Area #1	Area #2	Area #3	Area #4	Area #5	Area #6
FL-I	84.0868	38.8548	67.9353	36.5578	67.9839	36.5578
FL-PI	83.9550	38.5150	67.6067	36.3980	67.8045	36.3980
FL-PID	90.1321	41.9895	72.8183	41.5722	81.5888	43.5064

Table 3. Comparison of the settling times, in percent; the given frequency tolerance is 0.1%. The settling times of the PI-based FL controller are much smaller than those of the other controllers to verify its dominant features.

Controller	Area #1	Area #2	Area #3	Area #4	Area #5	Area #6
FL-I	34.2532	82.3184	33.1244	15.1310	22.8100	21.7496
FL-PI	39.2220	82.8078	39.1683	19.0005	25.2363	27.3118
FL-PID	64.9606	98.2616	73.4166	40.6910	50.5558	58.4901

5. Discussion and conclusion

A typical model of a 6-control-area nonreheat interconnected power system has been designed in this work to deal with the frequency control strategy against load variations. In addition, different controllers (I, PI, PID, and PI-based FL) based on the tie-line bias control scheme have been analyzed in order to maintain the frequency and tie-line power flow at the nominal value and scheduled power, respectively. The obtained simulation results demonstrate clearly the effectiveness of the PI-based FL controllers to solve the problem of frequency stability in comparison with the other regulators. For future work, the proposed PI-based FL controllers will be combined with other modern techniques, e.g., artificial neural network (ANN), to adapt more effectively to the diversity and complexity of large-scale power systems in reality. In principle, this modern control technique can be used to automatically tune the correct gain factors of the corresponding FL controllers. Furthermore, practical large-scale power systems, such as Sichuan's electric grid in China, should be of interest to model. The improved control strategies will then be applied to this model to ensure the stability, efficiency, and economy during the actual working process of the power system.

Acknowledgment

This work was supported by the Natural Science Foundation of China (NSFC, Grant No. 51277022) and the Fundamental Research Funds for the Central Universities (ZYGX2009J069).

Nomenclature

i	index of the control area $\#i$, $i = 1, 2, 3, 4, 5, 6$
f_n	nominal frequency, $f_n = 50$ Hz
f	real frequency of the network, Hz
$P_{tie,i}$	tie line power flow, pu
$\Delta f_i(t)$	frequency deviation, in time domain, pu
$\Delta F_i(s)$	frequency deviation, in Laplace domain, pu
ΔP_{Di}	load variation, pu
$\Delta P_{tie,i}$	tie-line power flow deviation, pu
T_{Gi}	time constant of governor, sec
T_{TGi}	time constant of nonreheat turbo-generator unit, s
K_{pi}	gain of power system, $Hz/pu.MW$
T_{pi}	time constant of power system, s
T_{ij}	tie-line time constant, s
B_i	frequency bias factor, $MW/pu.Hz$
R_i	speed regulation factor, $Hz/pu.MW$

References

[1] Kundur P. Power System Stability and Control. New York, NY, USA: McGraw-Hill, 1994.

[2] Murty PSR. Operation and Control in Power Systems. Hyderabad, India: BS Publications, 2008.

[3] Shashi KP, Soumya RM, Nand K. A literature survey on load-frequency control for conventional and distribution generation power systems. Renewable and Sustainable Energy Reviews 2013; 25: 318–334.

[4] Subbaraj P, Manickavasagam K. Generation control of interconnected power systems using computational intelligence techniques. IET Gener T Distrib 2007; 1: 557-563.

[5] Kocaarslan İ, Çam E. Fuzzy logic controller in interconnected electrical power systems for load-frequency control. Electrical Power and Energy System 2005; 27: 542-549.

[6] Wen T, Hong Z. Robust analysis of decentralized load frequency control for multi-area power systems. Electrical Power and Energy Systems 2012; 43: 996-1005.

[7] Ateeth KT, Harikrishna N, Vigneesh P. Decentralized control of multi-area power system restructuring for LFC optimization. In: 2012 IEEE International Conference on Power Electronics, Drives and Energy Systems; 16–19 December 2012; Bengaluru, India: IEEE. pp. 106-112.

[8] Shayeghi H, Shayanfar HA. Application of ANN technique based on μ -synthesis to load frequency control of interconnected power system. Electrical Power and Energy Systems 2006; 28: 503-511.

[9] Panna R, Jha AN. Automatic generation control of interconnected hydro-thermal system in deregulated environment considering generation rate constraints. In: IEEE 2010 International Conference on Industrial Electronics, Control and Robotics; 2010; India: IEEE. pp. 148-159.

[10] Ali MY, Ayman AA. Effect of non-linearities in fuzzy approach for control a two-area interconnected power system. In: IEEE 2010 International Conference on Mechatronics and Automation; 4–7 August 2010; Xi'an, China: IEEE. pp. 706-711.

[11] Nanda J, Mangla A. Automatic generation control of an interconnected hydro-thermal system using conventional integral and fuzzy logic controller. In: IEEE 2004 International Conference on Electric Utility Deregulation, Restructuring and Power Technologies (DRPT2004); April 2004; Hong Kong, China: IEEE. pp. 372-377.

[12] Ogbonna B, Ndubisi SN. Neural network based load frequency control for restructuring power industry. Nigerian Journal of Technology (NIJOTECH) 2012; 31: 40-47.

[13] Mohammad AH, Abbas K, Mohammad J. Fuzzy based load frequency controller for multi area power system. Tech J Engin & App Sci 2013; 3: 3433-3450.

[14] Prakash S, Sinha SK. Application of artificial intelligence in load frequency control of interconnected power system. International Journal of Engineering Science and Technology 2011; 3: 264-275.

[15] Sharifi A, Sabahi K, Aliyari SM, Nekoui MA, Teshnehlab M. Load frequency control in interconnected power system using multi-objective PID controller. In: IEEE 2008 International Conference on Soft Computing in Industrial Applications (SMCia/08); 25–27 June 2008; Muroran, Japan: IEEE. pp. 217-221.

[16] Basilio JC, Matos SR. Design of PI and PID controllers with transient performance specification. IEEE T Educ 2002; 45: 364-370.

[17] Mann GKI, Hu BG, Gosine RG. Two-level tuning of fuzzy PID controllers. IEEE T Syst Man Cy B 2001; 31: 263-269.

[18] Visioli A. Tuning of PID controllers with fuzzy logic. IEE Proc Control Theory Appl 2001; 148: 1-8.

[19] Khodabakhshian A, Hooshmand R. A new PID controller design for automatic generation control of hydro power systems. Electrical Power and Energy Systems 2010; 32: 375-382.

[20] Khodabakhshian A, Edrisi M. A new robust PID load frequency controller. Control Engineering Practice 2008; 16: 1069-1080.

[21] Qing GW, Tong HL, Ho WF, Qiang B, Yu Z. PID tuning for improved performance. IEEE T Contr Syst T 1999; 7: 457-465.

[22] Hamed S, Behrooz V, Majid E. A robust PID controller based on imperialist competitive algorithm for load-frequency control of power systems. ISA Transactions 2013; 52: 88-95.

[23] Wen T. Unified tuning of PID load frequency controller for power system via IMC. IEEE T Power Syst 2010; 25: 341-350.

[24] Saravuth P, Issarachai N. Optimal fuzzy logic-based PID controller for load-frequency control including superconducting magnetic energy storage units. Energy Conversion and Management 2008; 49: 2833-2838.

[25] Chandrakala KRMV, Balamurugan S, Sankaranarayanan K. Variable structure fuzzy gain scheduling based load frequency controller for multi source multi area hydro thermal system. Electrical Power and Energy Systems 2013; 53: 375-381.

[26] Hassan MAM, Malik OP. Implementation and laboratory test results for a fuzzy logic self-tuned power system stabilizer. IEEE T Energy Conver 1993; 8: 221-228.

[27] Bimal KB. Modern Power Electronics and AC Drives. Upper Saddle River, NJ, USA: Prentice Hall PTR, 2002.

Appendix

6-control-area interconnected power system parameters.

$T_{G1} = 0.08,\ T_{G2} = 0.12,\ T_{G3} = T_{G4} = T_{G5} = T_{G6} = 0.1$

$T_{TG1} = 0.3,\ T_{TG2} = 0.3,\ T_{TG3} = T_{TG4} = T_{TG5} = T_{TG6} = 0.35$

$K_{p1} = 120,\ K_{p2} = 100,\ K_{p3} = K_{p4} = K_{p5} = K_{P6} = 98$

$T_{p1} = 18,\ T_{p2} = 20,\ T_{p3} = T_{p4} = T_{p5} = T_{p6} = 25;\ T_{ij} = 0.071$